

Objectives

- Introduce a height profiling technique for thermospheric winds to address the gap between 100 km and 150 km where measurement techniques are limited.
- Using this height profiling technique, show that the cusp region density enhancement has no predominant effects on neutral wind signatures lower than 240 km altitude.

Motivation

Few techniques are available for measuring neutral winds at E-region altitudes ranging from 100 to 150 km (Figure 1). In-situ probes are typically unable to remain aloft at these heights for more than a few hours, and remote sensing is largely ineffective. The consequent scarcity of observations is a problem because winds in this region are of scientific and operational interest. This coupling altitude region is the transition from atmospheric behavior to space-like behavior where solar ultraviolet radiation is absorbed, semi diurnal tides driven from below dissipate, radio signals can be impacted, etc. Further, strong altitude gradients of wind and temperature are known to occur at these heights, so any useful measurement techniques must account for these gradients and, ideally, resolve them.

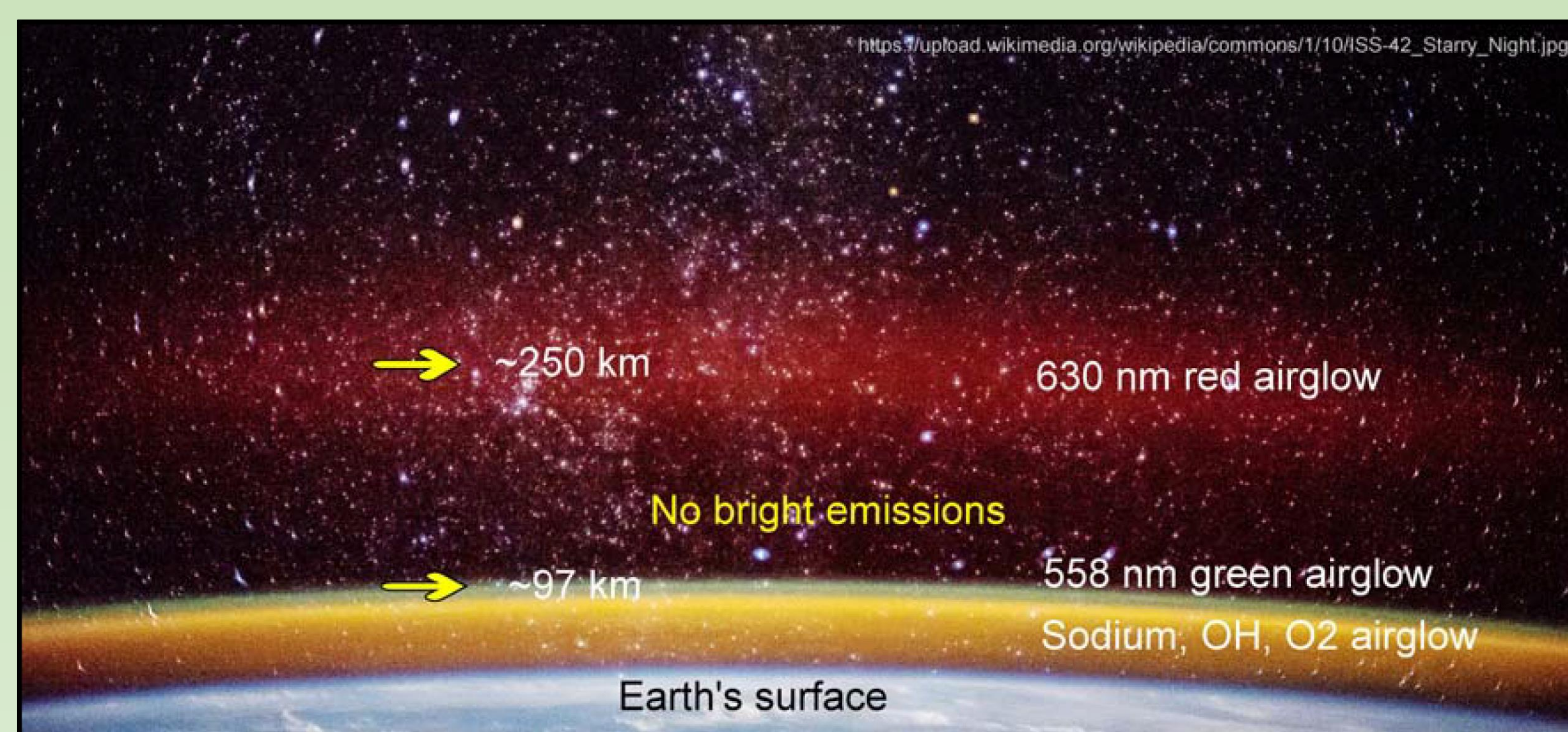


Figure 1: Airglow emissions in the thermosphere and the lack of emissions between ~100 km to ~250 km. Auroral activity from oxygen 558 nm emissions can, at times, narrow the gap. Since auroral emissions are much brighter than airglow, measurement techniques are unaffected by airglow during these times.

Scanning Doppler Imagers (SDI) are ground-based, all-sky imaging Fabry-Perot spectrometers that allocate zones across the sky to record Doppler spectra of emissions, shown in Figure 2. By numerically fitting profiles to sky spectra, a Doppler shift and Doppler temperature can be derived. These instruments have been described in detail previously by Conde and Smith (1995)¹. Aurorally excited 558 nm and 630 nm emissions from atomic oxygen are used to map neutral winds at altitudes around 120 km and 240 km respectively. When the aurora is present, the characteristic energy of electron precipitation within the aurora can change by many keV on time scales of minutes or less. As a result, 558 nm emission heights may vary between 95 and 150 km both across the sky and over time.

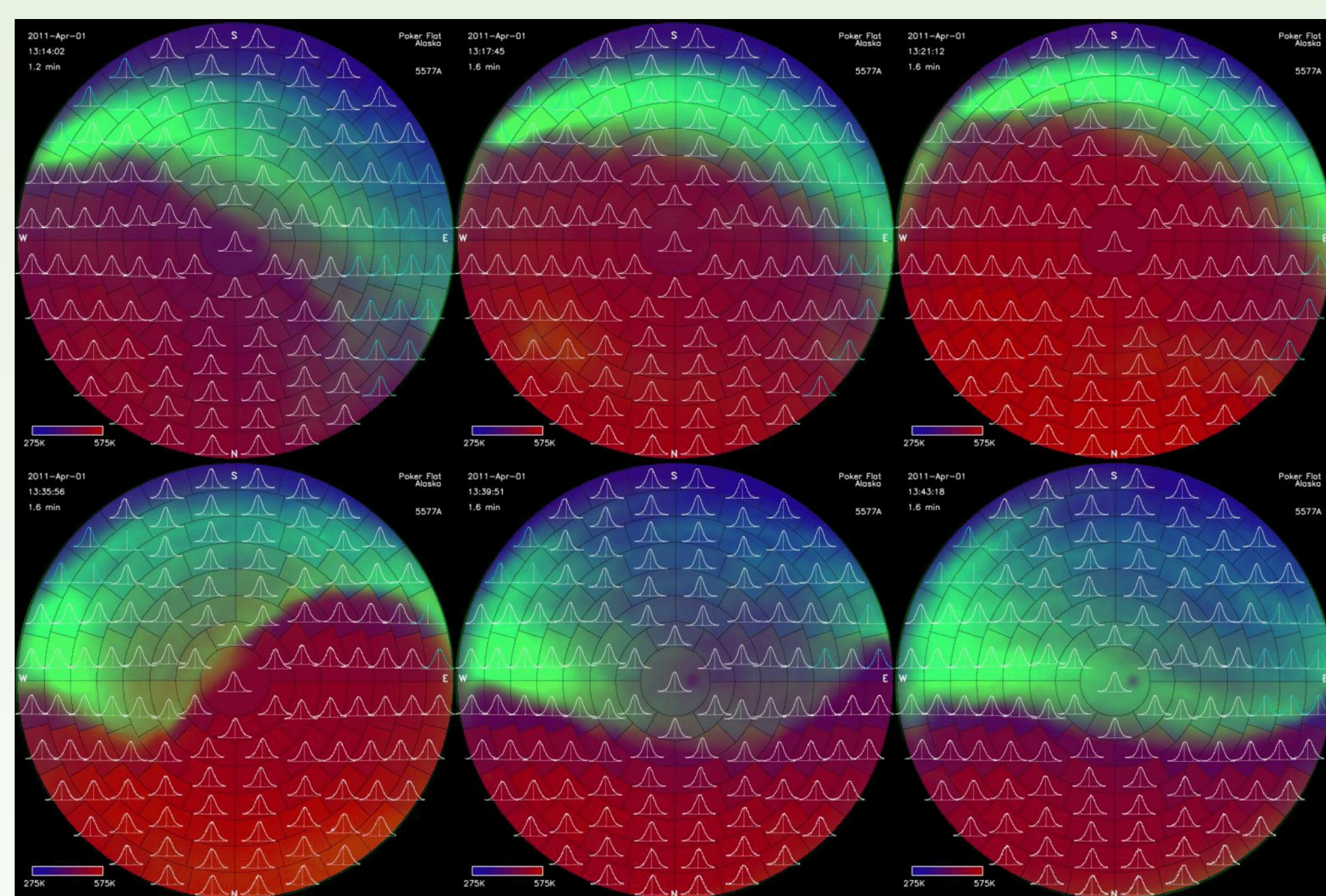


Figure 2: SDI 558nm data from April 1st, 2011 at Poker Flat, Alaska showing auroral intensity in green, temperature at emission height in red and blue, and original spectra in white “bell” curves. Temperature changes seen are largely due to the changing emission altitude. Note the transition from warmer poleward temperatures to colder equatorward temperatures lying under strong auroral intensity implying higher characteristic energies.

This behavior coupled with altitude gradients in the wind field would violate the assumptions usually used to reconstruct wind vectors producing noisy and unphysical results. However, rather than disregarding these periods, it is possible to instead make use of the height variations to construct an altitude profile of wind.

Height Profiling

The MSIS atmosphere model predicts the height profile of temperature for the night by using the prevailing F10.7 and Ap values. This profile is used to assign a height to each 558 nm spectrum by comparing the fitted Doppler temperature to the MSIS model’s prediction. Outcomes of this process are shown in Figure 3. During times when these observations span a range of heights, it is possible to invert the line-of-sight wind components to create a height profile of the two-component horizontal vector wind. Results from this height profiling technique have been shown to agree with absolute measurements of wind using a chemical release from sounding rocket missions shown in Figure 4.

References

- ¹Conde, M., and R. W. Smith. “Mapping thermospheric winds in the auroral zone.” *Geophysical research letters* 22.22 (1995): 3019-3022.
- ²Larsen, Miguel. Rocket Wind Profiles. 2017.
- ³Liu, H., et al. “Global distribution of the thermospheric total mass density derived from CHAMP.” *Journal of Geophysical Research: Space Physics* 110.A4 (2005).
- ⁴Schlegel, Kristian, et al. “Thermospheric density structures over the polar regions observed with CHAMP.” *Annales Geophysicae*. Vol. 23. No. 5. 2005.

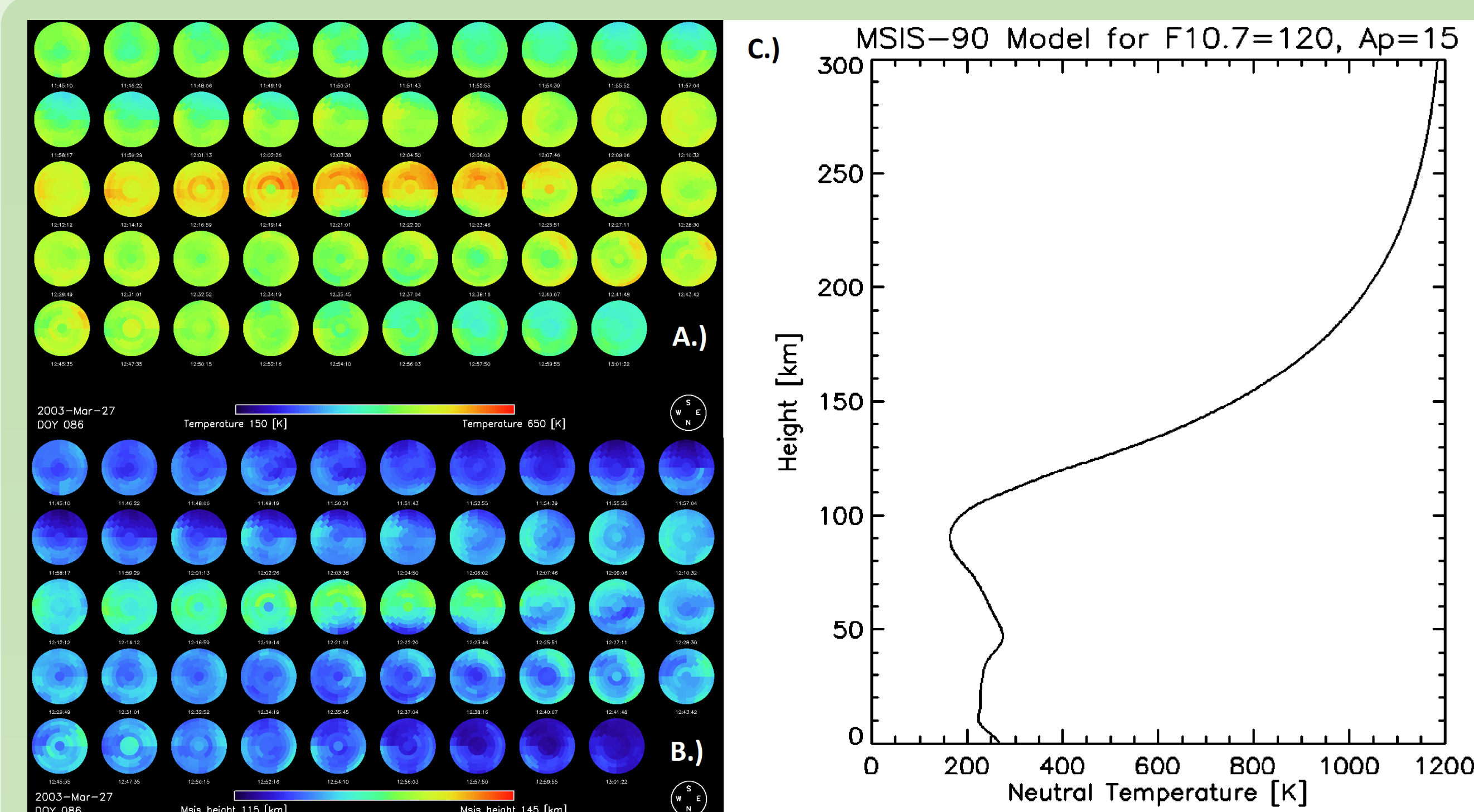


Figure 3: A.) Time evolving temperature sky maps derived from the Poker Flat SDI on the night of the JOULE sounding rocket launch March 27th 2003. B.) Time evolving calculated MSIS height maps over the same time period. Note that similarities in temperature and height distributions occur because temperatures from 3A are used to assign altitudes in 3B. C.) Example MSIS height profile to demonstrate the swiftly changing temperature with altitude.

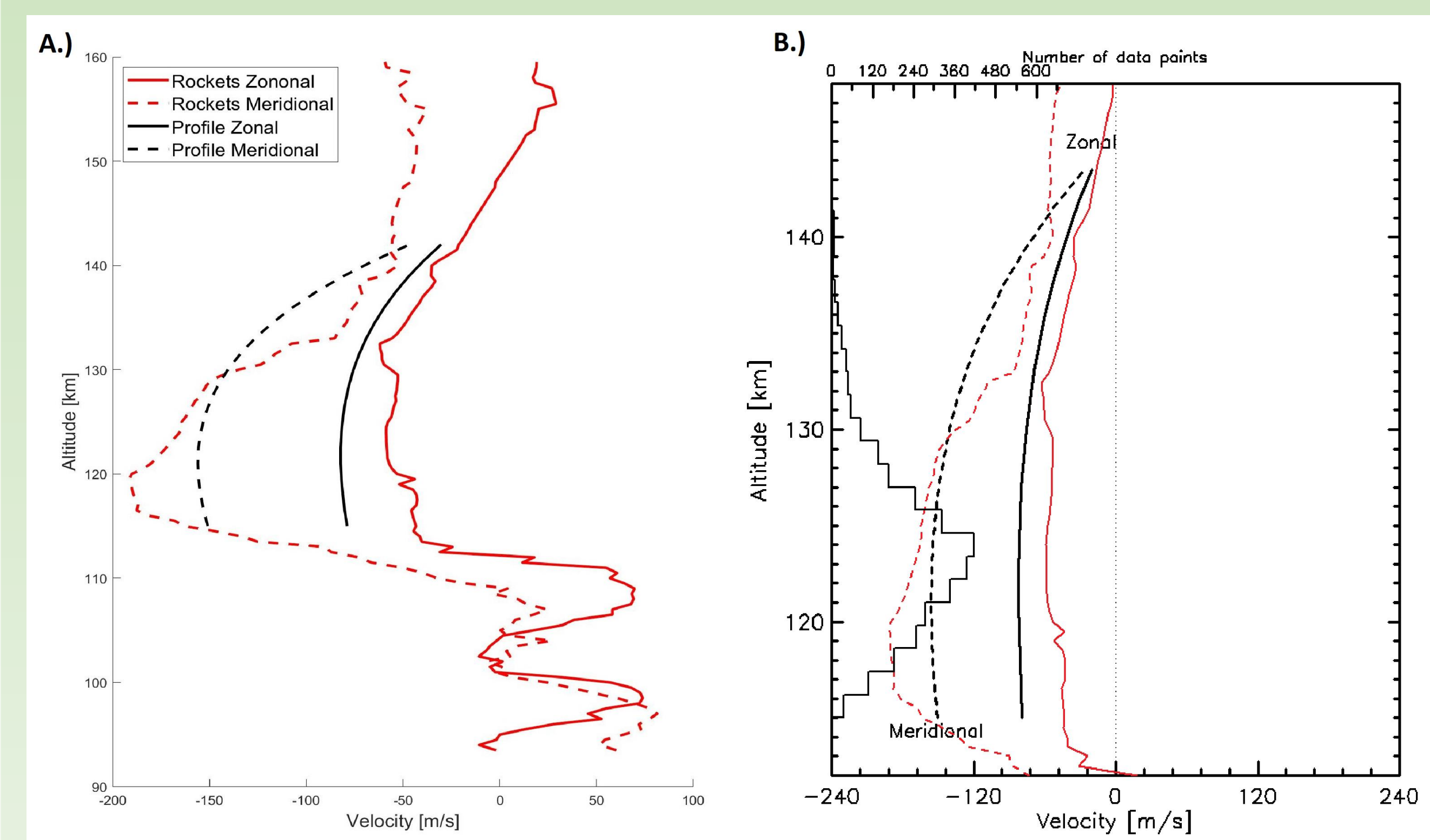


Figure 4: Zonal and meridional component comparison of absolute wind measurements from the JOULE rocket TMA release at 12:13 UT (red) with height profiling technique results (black). 4A shows the full altitude range of the rocket profile versus the limited range of the height profiling technique. 4B emphasizes technique profiles and shows the histogram of data points contributing to each altitude. Note that even though the histogram is very skewed towards lower altitudes, the agreement with absolute measurements is still present throughout the height profile.

Cusp Density Enhancement

At the start of the 2000’s, satellite accelerometer observations at about 400 km altitude showed a persisting and significant increase in neutral particle density near the geomagnetic cusps described thoroughly by Liu et al.³ and Schlegel et al.⁴. Data shows that this density anomaly (Figure 5) is stable, which means must be continuously supported against gravity. Background atmosphere in this region is supported by hydrostatic equilibrium such that force from the vertical pressure gradient is balanced by force of gravity ($\frac{\partial P}{\partial z} = -\rho g$). One mechanism for supporting the additional mass within the density anomaly would be modifying the preexisting hydrostatic equilibrium by introducing a local perturbation to the vertical pressure gradient in the anomaly. However, this also introduces a change in the horizontal pressure gradient that would, inevitably, drive very large local wind perturbations (at least 500 m/s.) Effects of these perturbations would penetrate below the 400 km altitude of the density enhancement, and be easily observed, if they exist.

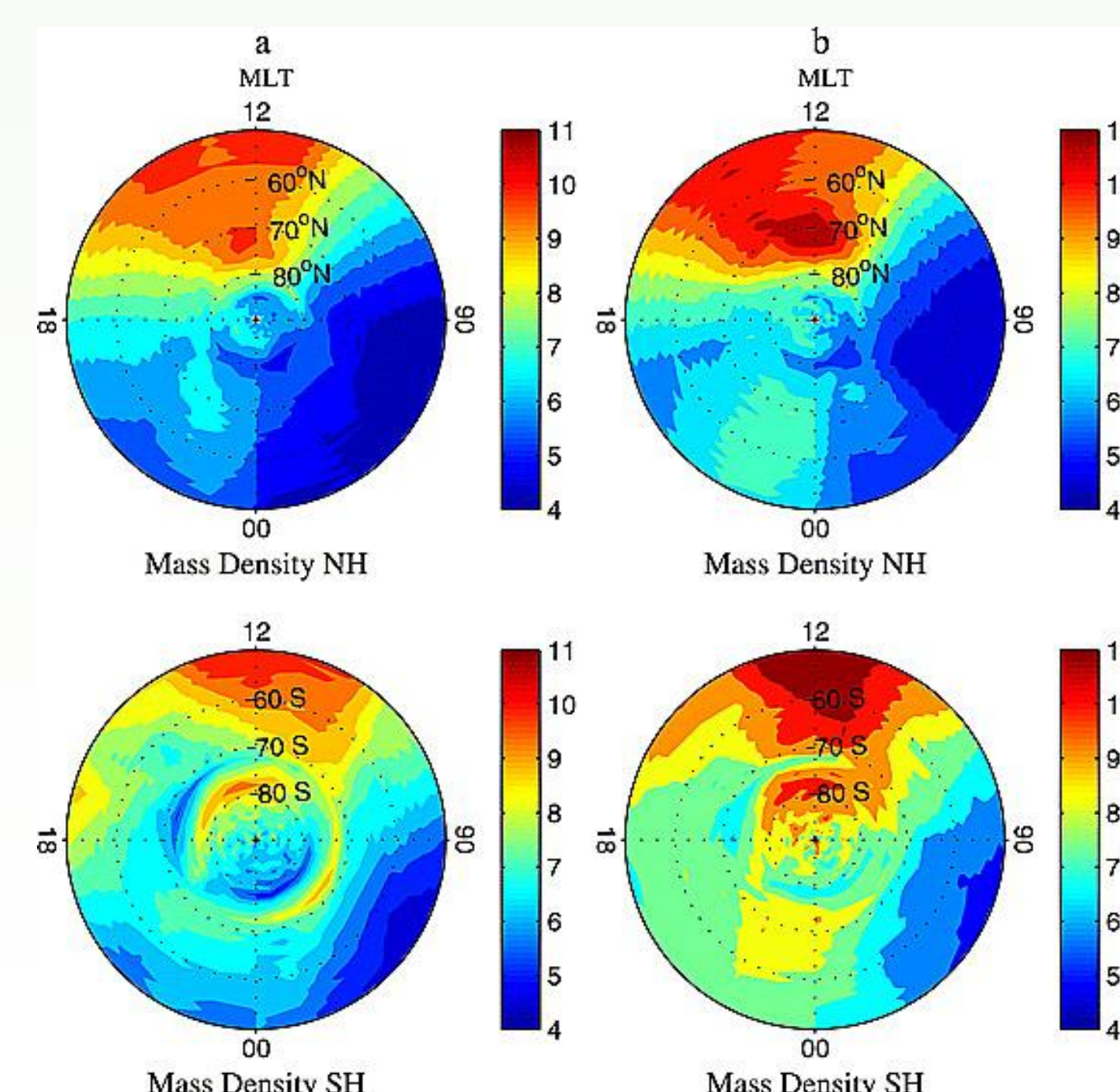


Figure 5: Density (in units of $10^{-12} \text{ kg m}^{-3}$) as seen over the poles for the northern (NH) and southern (SH) hemispheres. 5a is data taken during quiet geomagnetic conditions and 5b is during moderately disturbed geomagnetic conditions. Note the density increase in all cases at magnetic noon (at the footprint of the cusp).³

Results

The height profiling technique that was introduced was shown to yield relevant results using data from Alaska. Further, this technique can be used on observations from two SDI sites in Antarctica: South Pole Station and McMurdo Station. These instrument locations fall within the footprint of the cusp region for a few hours each night. Making comparisons from before, during, and after the cusp region passes over two observational sites shows that no significant signatures are introduced into the wind profiles while the density enhancement is over the observation sites.

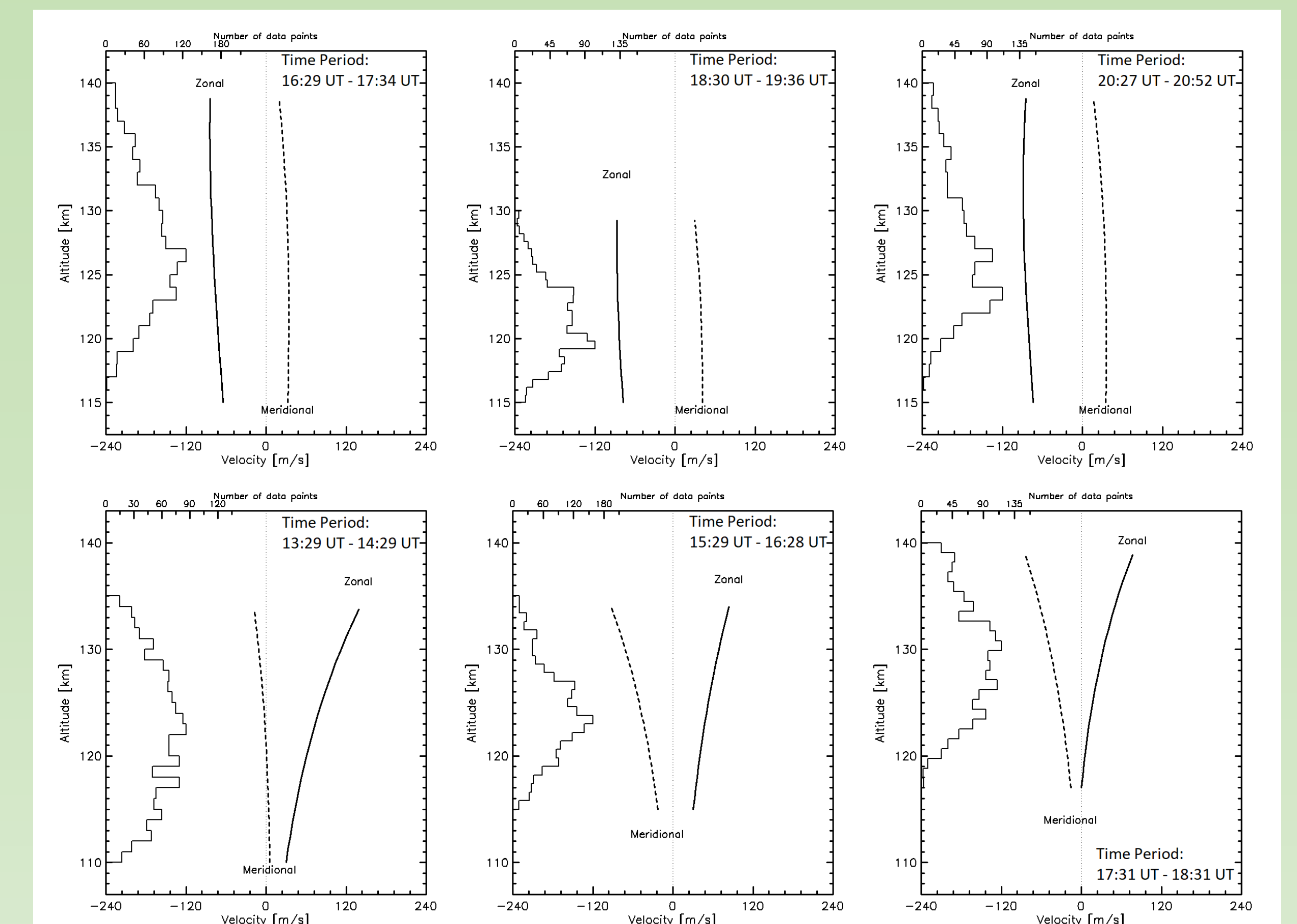


Figure 6: Height profiles generated from McMurdo (top) and South Pole (bottom) for approximately 1 hour periods centered around times before (left), during (middle), and after (right) cusp passing. Despite varying emission altitude and therefore characteristic energy, the profiles maintained the same general shape throughout the passing of the cusp.

Conclusions from results shown in Figure 6 are limited to the height ranges available to model with this technique, and thus only range up to 150 km. Since the density enhancement in the cusp is at altitudes of 400 km, this technique alone is most likely focused on altitudes below where the largest wind effects would manifest. However, the 630 nm oxygen emission can be used to find if any perturbations are observed at altitudes up to 240 km. By generating time evolving wind field plots for 630 nm oxygen emissions, any changes due to the density enhancement would be detected. As seen in Figure 7, no obvious signatures are apparent during the passing of the cusp.

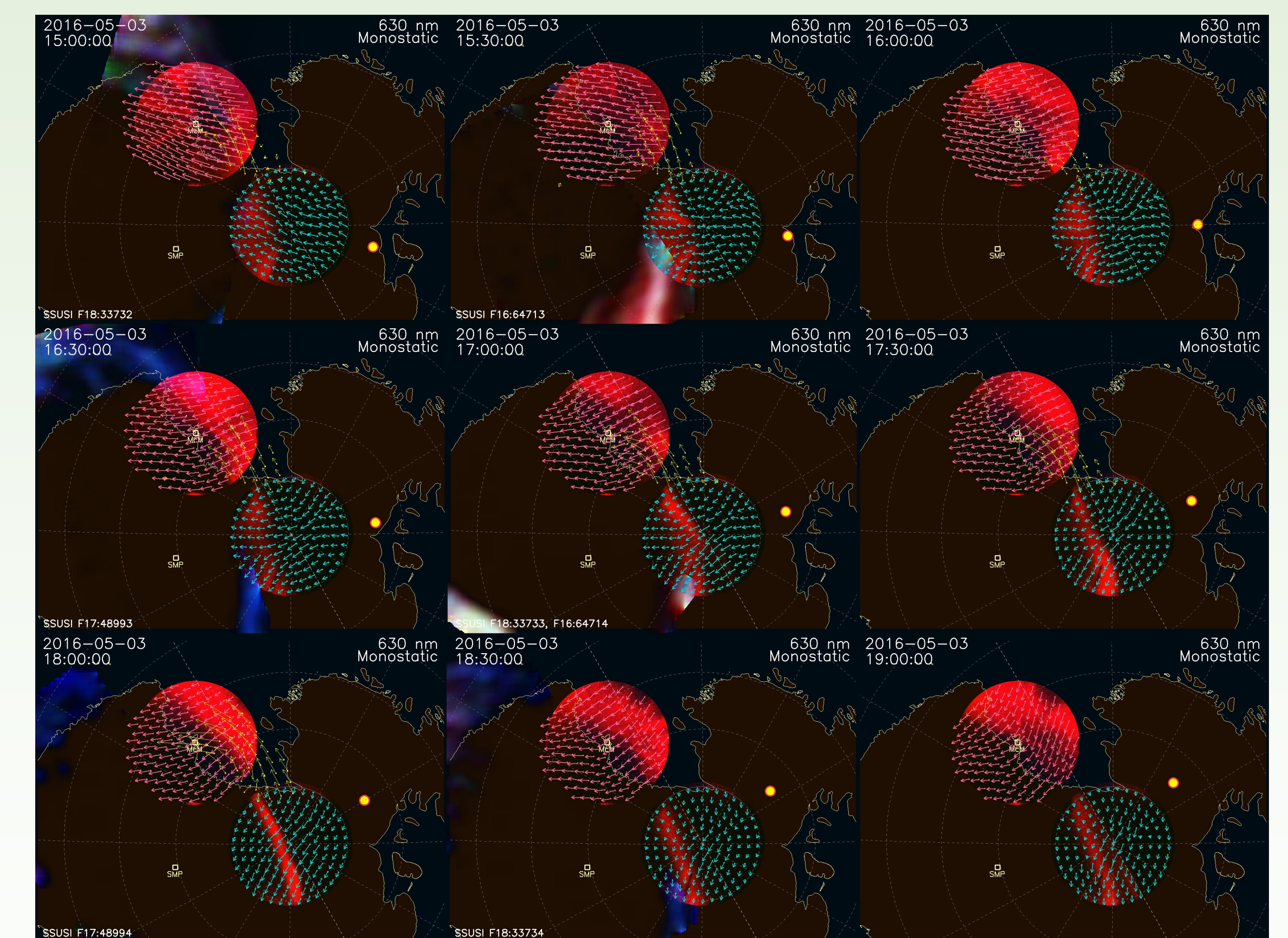


Figure 7: Wind fields from oxygen 630 nm emissions over South Pole (blue) and McMurdo (red) stations. Note no predominant changes in the wind fields exist over time. Also shown are FPI images from the locations, SSUSI F17 images, and SuperDARN data (yellow).

Conclusions

Despite the lack of any wind defects found in neutral winds lower than 240 km, not all is lost. The unphysically large winds that would be produced by hydrostatic equilibrium modifications would have penetrating effects at the altitudes examined. Since no perturbations are observed, it suggests that another explanation is required for support of the enhanced mass. Additionally, this study aids in limiting the altitude range in which these signatures are present, consequently restricting where the supporting mechanism for the density enhancement occurs. Research advances towards finding the support mechanism or any effects of it will most likely be found between 240 km and 400 km or above 400 km. Results also suggest that the density enhancement may have more of an impact on satellite orbits and communication by being present at higher altitudes. Below 240 km, satellites are unlikely to spend much time and would not have to be as concerned with wind perturbations. However, the probable presence of wind defects in an altitude range where satellites do orbit makes the search for an answer more important.